Report of Visiting Scientist mission NWP_VS18_03

Document NWPSAF-EC-VS-029

Version 1.0

29-07-20

Comparisons of ocean radiative transfer model simulations with GMI observations, between 10 and 170 GHz

Lise Kilic

Observatoire de Paris - Laboratoire d'Etudes du Rayonnement et de la Matière en Astrophysique et Atmosphères (LERMA), 61 Avenue de l'Observatoire, 75014 Paris, France

Comparisons of ocean radiative transfer model simulations with GMI observations, between 10 and 170 GHz

Lise Kilic (LERMA)

This documentation was developed within the context of the EUMETSAT Satellite Application Facility on Numerical Weather Prediction (NWP SAF), under the Cooperation Agreement dated 7 December 2016, between EUMETSAT and the Met Office, UK, by one or more partners within the NWP SAF. The partners in the NWP SAF are the Met Office, ECMWF, DWD and Météo France.

Change record			
Version	Date	Author / changed by	Remarks
0.1	07/20	L. Kilic	Draft version
0.2	07/20	L. Kilic	Incorporated comments from C. Prigent and S. English
1.0	29/07/20	L. Kilic	Final version

Associate scientist mission NWP_AS18_P03 report: Comparisons of ocean radiative transfer model simulations with GMI observations, between 10 and 170 GHz

Lise Kilic

July 29, 2020

1 Introduction

Observation of the ocean is important for oceanic forecasting, numerical weather prediction (NWP), oceanic circulation, mesoscale analysis, and for the study and modeling of climate change. To characterize the ocean surface, an ocean Radiative Transfer Model (RTM) is required to interpret the measurements of the satellite instruments. Generally, ocean RTMs use three fundamental variables as inputs to simulate a sea surface emissivity: the sea surface temperature (SST), the sea surface salinity (SSS), and the ocean wind speed (OWS).

The 21^{st} international TOVS study conference recommended to the community the development of a reference quality ocean surface emissivity model from microwave to infrared for both passive and active simulations. An international working group has been put in place within the International Space Science Institute (ISSI) in Switzerland, to discuss and develop such a reference sea surface emissivity model (https://www.issibern.ch/teams/oceansurfemiss/).

In this study we will contribute to this effort by comparing the simulations of three well known ocean radiative transfer models (RTMs) in microwave with the Global Precipitation Measurement (GPM) Microwave Imager (GMI) observations. Three ocean RTMs are selected for this study: a physically-based model, LOCEAN [Dinnat et al., 2003, Yin et al., 2016], a fast model derived from a physically-based model, FASTEM [English and Hewison, 1998, Liu et al., 2011], and an empirical model fitted to satellite observations, RSS [Meissner and Wentz, 2004, 2012]. In a previous study, ocean RTM simulations have been compared with Soil Moisture Active Passive (SMAP) and Advanced Microwave Scanning Radiometer 2 (AMSR2) observations [Kilic et al., 2019]. That study focused especially on low frequencies between 1.4 and 36.5 GHz. Here, in this new analysis we propose to compare the ocean RTM simulations with GMI observations, from 10 to 183 GHz. The first goal of this study is to evaluate the potential of the LOCEAN model to be used as the basis for the development of the reference microwave sea surface emissivity model. We will identify where are the needs to adapt this model for its use over a larger range of conditions.

In Section 2, the necessary data for the analysis are presented. In Section 3, the methodology and the RTMs adopted for this study are described. Section 4 presents the results of the comparison between GMI observations and the RTM simulations. In Section 5, we discuss the possibilities of improvement of the ocean RTMs. Finally, Section 6 concludes this study.

2 Data

2.1 GMI Observations

The GMI instrument onboard GPM satellite is a dual-polarization, multi-channel, conical-scanning, passive microwave radiometer. It observes at frequencies from 10 to 183 GHz (see Table 1). It is a well calibrated instrument [Wentz and Draper, 2016] that makes it the best instrument for this study as the calibration issues will be minimal for the comparison with the simulations. For our analysis, three days (5, 15, and 25) of the months of January, April, July, and October in 2016 are selected. We use the GMI L1C-R products provided by NASA (https://pmm.nasa.gov/data-access/downloads/gpm, ftp: arthurhou.pps.eosdis.nasa.gov). It contains the GMI brightness temperatures (TBs) from 10 to 183 GHz collocated on the same swath.

Table 1: GMI channels from http://www.remss.com/missions/gmi/.

Frequency (GHz)	Polarization	Spatial Resolution (km×km)
10.65	V,H	32×19
18.7	V,H	18×11
23.8	V	16×10
36.5	V,H	15×9
89	V,H	7×4
166.5	V,H	6×4
183±3	V	6×4
183±7	V	6×4

2.2 Geosphysical Inputs

The GMI observations are collocated with surface and atmospheric parameters from the European Centre for Medium-Range Weather Forecasts (ECMWF) Re-Analysis ERA5 and from the Mercator Ocean reanalysis (Global Analysis Forecast Phy 001 024 distributed by the Copernicus Marine Service, Lellouche et al. [2019]). We use ERA5 data on pressure levels for the atmospheric fields, and on single level for surface parameters, both at 0.25° of spatial resolution, and the information is available hourly. ERA5 provides the pressure, temperature, specific humidity, and liquid water content atmospheric profiles to run the atmospheric RTM, and the sea surface temperature (SST), and the ocean wind speed (OWS) to run the ocean RTMs. The Mercator data at 0.083° spatial resolution and daily average are selected to provide the sea surface salinity (SSS) needed to run the ocean RTMs. The collocation with GMI data is performed with nearest neighbor interpolation, spatially, and temporally.

3 Method

3.1 Selected Ocean Radiative Transfer Models

The microwave ocean emissivity varies with SST, OWS, and SSS, with sensitivities that depend upon the frequency, the polarization, and the incidence angle of observation [Wilheit and Chang, 1980]. There are essentially three classes of emissivity models. Firstly, there are physical models, although some of their components may be empirically tuned: they tend to rigorously represent the complex physical interactions between the ocean surface and the radiation and are generally rather slow. Secondly, there are fast models that attempt to replicate the results of the previous physical models, using parameterizations. Lastly, there are empirical models, partly derived from matchups between in situ ocean observations and satellite observations.

Usually, an ocean RTM has three main components: 1) a dielectric sea water model, 2) a roughness model, and 3) an ocean foam model. The dielectric constant needed to simulate the emissivity of a flat surface depends on the SST, the SSS, and the frequency. Dielectric constant models are expressed as a Debye law [Debye, 1929] with coefficients adjusted to observations. Some dielectric constant models use a double Debye formula to extend the range of frequencies where the model is valid. A roughness model is then needed to simulate the effect of the wind-induced roughness on the ocean. Here, different types of model can be applied. The geometric optic models consider the large scale waves as an ensemble of facets with different slopes for which the Fresnel reflection applies. The double scale models consider the scattering by the small-scale roughness on each large-scale wave, in addition to the large scale model. Then, when the steepness of the waves is too large, the waves break, and foam appears. The presence of foam is characterized by 1) a foam cover that depends upon the OWS and is usually written as a power law of he OWS [Monahan and O'Muircheartaigh, 1980], and 2) a foam emissivity that depends upon the frequency and incidence angle.

In this study, three ocean RTMs are compared. They are representative of the three model classes:

- The Laboratoire d'Océanographie et du Climat (LOCEAN) RTM is a full physical model. Special efforts have been carried out to adjust it to L-band observations (SMOS and SMAP). It was implemented by Emmanuel Dinnat and Xiaobin Yin at LOCEAN [Dinnat et al., 2003, Yin et al., 2016]. It is derived from the two-scale model of Yueh [1997]. The dielectric constant stems from Klein and Swift [1977], the roughness model uses the wave spectrum from Durden and Vesecky [1985] with an amplitude coefficient a_0 of the wave spectrum multiplied by 1.25 [Yin et al., 2012]. The foam cover model follows Yin et al. [2016], and the foam emissivity model is from Anguelova and Gaiser [2013]. This model was primarily designed for the analysis of SMOS L-band observations. Its physical basis is nevertheless generic and makes it applicable to a large range of frequencies.

- The FAST microwave Emissivity Model (FASTEM) is a fast linear regression fit to the output of a physical two scale model [English and Hewison, 1998, Liu et al., 2011]. It is distributed with the RTTOV, the community radiative transfer code [Saunders et al., 1999, 2018]. It was primarily developed for the assimilation of surface-sensitive microwave satellite observations in NWP centers, at frequencies above 6 GHz. FASTEM version 5 is used here. The fast linear regression fits the output of a physical two scale model in which the dielectric constant model is described in Liu et al. [2011], derived from the permittivity model of Ellison et al. [1998] and adapted with a double Debye relaxation. The roughness model is based on the wave spectrum of Durden and Vesecky [1985] with an amplitude coefficient a_0 of the wave spectrum multiplied by 2 [Yueh, 1997]. The foam cover model is from Monahan and O'Muircheartaigh [1986]. The foam emissivity is described in Liu et al. [2011]: it is a combination of the adjustments of Kazumori et al. [2008] and Stogryn [1972].

- The Remote Sensing Systems (RSS) model is essentially fitted to satellite observations. It is developed with SSM/I and WindSat observations between 6 and 89 GHz [Meissner and Wentz, 2004, 2012] and with Aquarius observations at 1.4 GHz [Meissner et al., 2014, 2018]. For the flat sea surface emissivity, it adopts the dielectric constant model of Meissner and Wentz [2004], adjusted in Meissner and Wentz [2012]. The wind-induced emissivity is fitted to satellite observations and described by a polynomial function: it includes the roughness model as well as the foam contribution. For the RSS model, there are two wind-induced emissivity parameterizations: one between 6 and 90 GHz based on SSM/I F13 and WindSat observations [Meissner and Wentz, 2012], and one at 1.4 GHz based on Aquarius observations [Meissner et al., 2014, 2018]. Note that the RSS model is not expected to work above 100 GHz.

Table 2: Summary of the selected ocean Radiative Transfer Models (RTMs).

RTM	Model type	Dielectric constant	Wave spectrum	Foam cover	Foam emissivity
LOCEAN Dinnat et al., 2003	Full physical model (adjusted for L-band)	Klein and Swift, 1977	Durden and Vesecky, 1985 with $a_0 \times 1.25$	Yin et al. 2016	Anguelova and Gaiser, 2013
FASTEM Liu et al., 2011	Parameterized and fast	Ellison et al., 1998 +Double Debye	Durden and Vesecky, 1985 with $a_0 \times 2$	Monahan and O'Muircheartaigh 1986	Kazumori et al., 2008 with Stogryn,1972
RSS Meissner and Wentz, 2012	Empirically fitted to observations	Meissner and Wentz, 2004 and 2012	Wind induced emissivity fitted to observations Meissner and Wentz, 2012 Meissner et al., 2014		

3.2 Atmospheric Radiative Transfer Model

The classic Rosenkranz model is used [Rosenkranz, 2017], with the latest improvements in atmospheric gas absorption as well as a formulation for the cloud liquid water non-scattering contribution. Note that RTTOV was used as the atmospheric RTM in the previous analysis in Kilic et al. [2019] with AMSR observations.

3.3 Filtering

First coastal areas are filtered out at 50 km from the coast to avoid contamination by land on ocean TBs.

GMI observations cover latitudes from 68°S to 68°N. Between these latitudes, the presence of sea ice is still possible. The sea ice areas are filtered out using the IceCream algorithm on the 18 and 36 GHz GMI channels [Kilic et al., 2020, Prigent et al., 2020]. As the algorithm is directly applied on the GMI observations, it makes the filtering more consistent and efficient.

GMI channels are up to 183 GHz. In this study, we compare GMI observations with the ocean RTM simulations from 10 to 166 GHz, the 183 GHz channels being located in a water vapor line with limited atmospheric transmission. The cloud impact on the observations increases with frequency, and an efficient cloud filtering has to be adopted, to avoid cloud contamination especially for frequencies above 40 GHz. A cloud classification has been developed by Favrichon et al. [2019], using GMI observations from 10 to 183 GHz to predict the pixel probability to be cloudy, following previous work by Aires et al. [2011]. Four different classes are separated: clear sky, low cloud, medium cloud, and high cloud. Here, we apply this classification and only keep the pixels belonging to the clear sky class.

4 Results

4.1 Systematic Errors

The systematic errors (i.e., the biases) are computed by averaging the difference between the TBs observed by GMI, and the TBs simulated with the ocean RTMs, for each channel and each model. The standard deviations of the differences between the observations and the simulations are also computed, noting that when looking at the histograms of the TB differences the distributions are gaussian (not shown here). Figure 1 illustrates the systematic errors with GMI observations. For comparison we show in Figure 2 the previous systematic error results obtained with SMAP and AMSR2 in Kilic et al. [2019].

The systematic error found with GMI are between -1.7 and 1.7 K for FASTEM, -1 and 1.5 K for RSS, and 0.4 and 3.6 K for LOCEAN. These biases are much lower than with AMSR2 observations. The GMI biases are larger for the horizontal polarization than for the vertical polarization, as expected, due to the lower sensitivity of the V polarization to the winds. The RSS model is the less biased ocean RTMs, and FASTEM is very close to the biases obtained with RSS. LOCEAN biases show that this RTM tends to underestimate the observed TBs. Despite the fact that the RSS has not been tuned to frequencies above 100 GHz, it does not show degraded performances at 166 GHz. Note that the LOCEAN model has been primarily adjusted for SMOS and SMAP applications at 1.4 GHz. Nevertheless, this is a physical model theoretically applicable to higher frequencies and it can benefit from some adjustments at higher frequencies.

4.2 Errors as a Function of Ocean Parameters

Figures 3 to 8 present the averaged differences between observed TBs and the simulated TBs (TBobs-TBsim) as a function OWS, SST, SSS, and TCWV for each channel of GMI up to 166.5 GHz. The number of observations used to compute the averaged differences is indicated by the grey histogram in the plots. These figures reproduce the same analysis as with AMSR2 and SMAP in Kilic et al. [2019].

The OWS dependence is the larger source of errors. For all frequencies, the differences between the simulations and the observations are relatively stable between 0 and 7 m/s. Above 7 m/s, the simulated TBs are underestimated with FASTEM and LOCEAN RTMs. The RSS model tends to overestimate the TBs for high wind speeds, especially for the H polarization. This can be explained by the fact that the RSS model has been fitted using wind speeds from the National Centers for Environmental Prediction General Data Assimilation System (NCEP GDAS) and on WindSat and SSM/I observations. For the analysis of the error dependence with the other parameters (SST and SSS), we select only the cases where the wind speed is between 0 and 7 m/s.

The errors as a function of SST are small (< 1 K for FASTEM and RSS) for the low frequencies (< 40 GHz). Note that the low frequencies (here, essentially the 10 GHz) are the most sensitive to SST. At higher frequencies, the sensitivity to water vapor becomes more important and can impact the results by its correlation to SST. The LOCEAN RTM shows larger errors especially at low SST, likely due to the dielectric constant model used in this RTM [Klein and Swift, 1977] that is adapted to low frequencies between 1 and 10 GHz.

At frequencies above 6 GHz, the TBs are not sensitive to SSS, therefore the error as the function of SSS is stable and lower than 1 K.

The error as a function of TCWV increases with frequency, as the sensitivity to the atmosphere increases with frequency. The errors are limited and very similar between the models as the same atmospheric RTM is adopted with all three surface. The small differences observed between the RTM are likely due to correlation between TCWV and SST. Comparisons in the water vapor line close to 23 GHz show little differences as a function of TCWV (Figure 5), confirming that the TCWV dependence is correctly simulated by the Rosenkranz atmospheric model, fed by the ECMWF water vapor profiles.

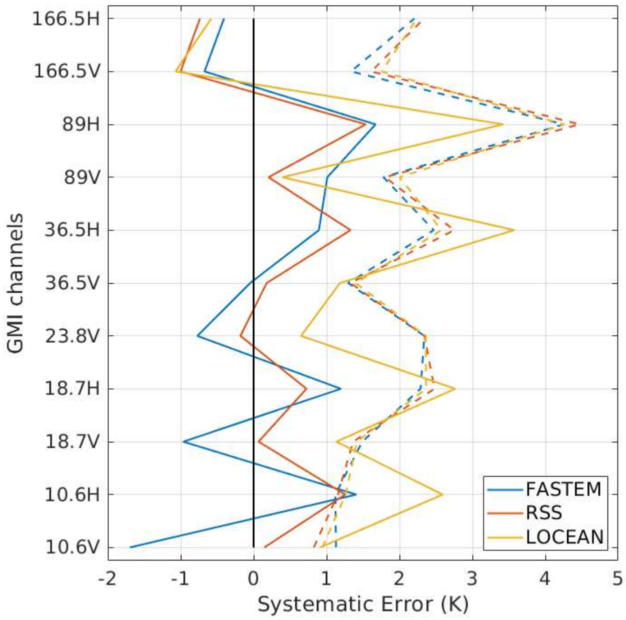

Figure 1: Systematic errors (TBobs-TBsim) for GMI channels from 10.65 to 166.5 GHz for the 3 ocean RTMs in solid lines, and the associated StD in dashed lines.

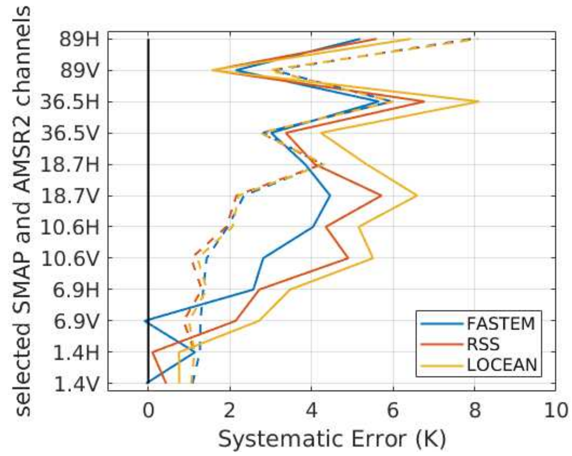

Figure 2: Systematic errors (TBobs-TBsim) for SMAP and AMSR2 channels from 1.4 to 89 GHz for 3 ocean RTMs in solid lines, and the associated StD in dashed lines. From Kilic et al. [2019].

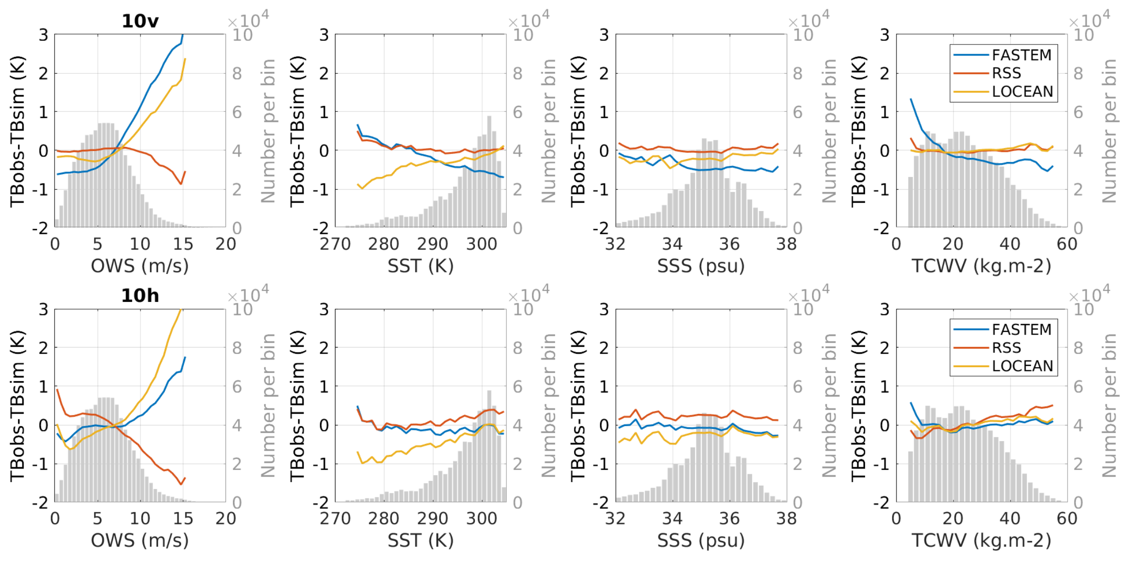

Figure 3: Errors (TBobs-TBsim) as a function of OWS (1^{st} column), SST (2^{nd} column), SSS (3^{rd} column), and TCWV (4^{th} column) for FASTEM, RSS, and LOCEAN models for the GMI 10.65 GHz channel in vertical (top) and horizontal (bottom) polarizations. For the error as a function of SST and SSS, the OWS is limited to 7 m/s.

To summarize, the two major sources of model errors are related to the OWS and SST dependences. For FASTEM, the larger errors are with OWS for high wind speed, especially at vertical polarization. For RSS, the larger errors are with OWS at high wind speed for the horizontal polarization. For LOCEAN, the larger errors are at OWS > 7 m/s, and for low SST, especially at high frequencies.

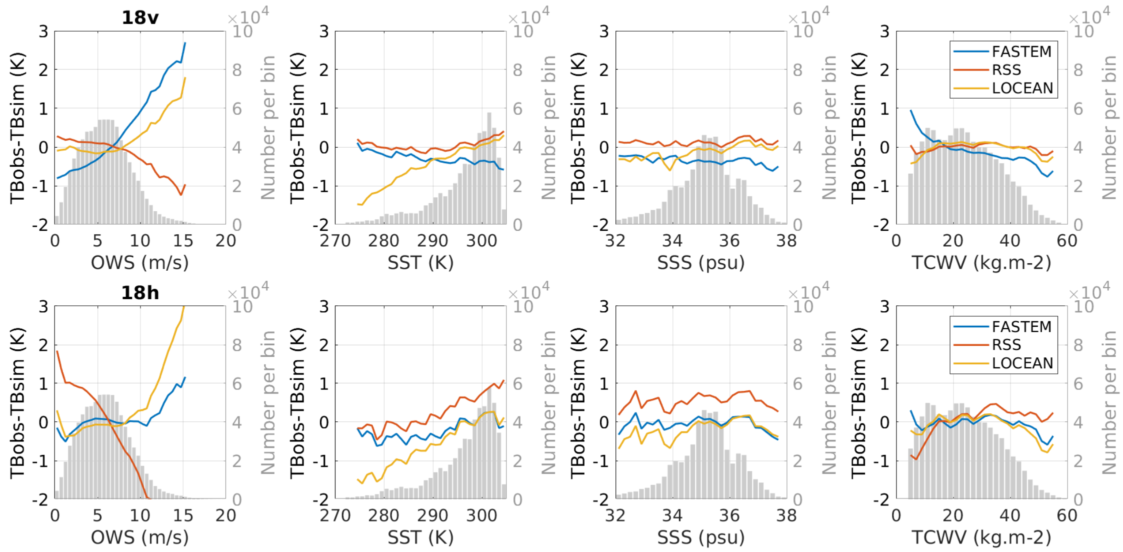

Figure 4: Same as Figure 3 but at 18.7 GHz.

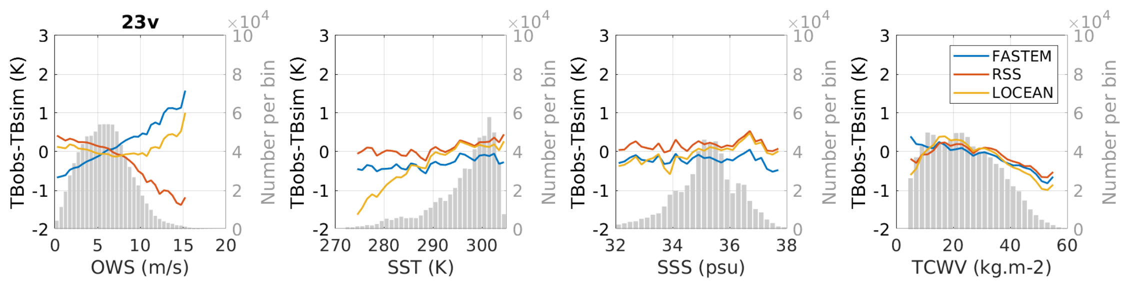

Figure 5: Same as Figure 3 but at 23.8 GHz in vertical polarization only.

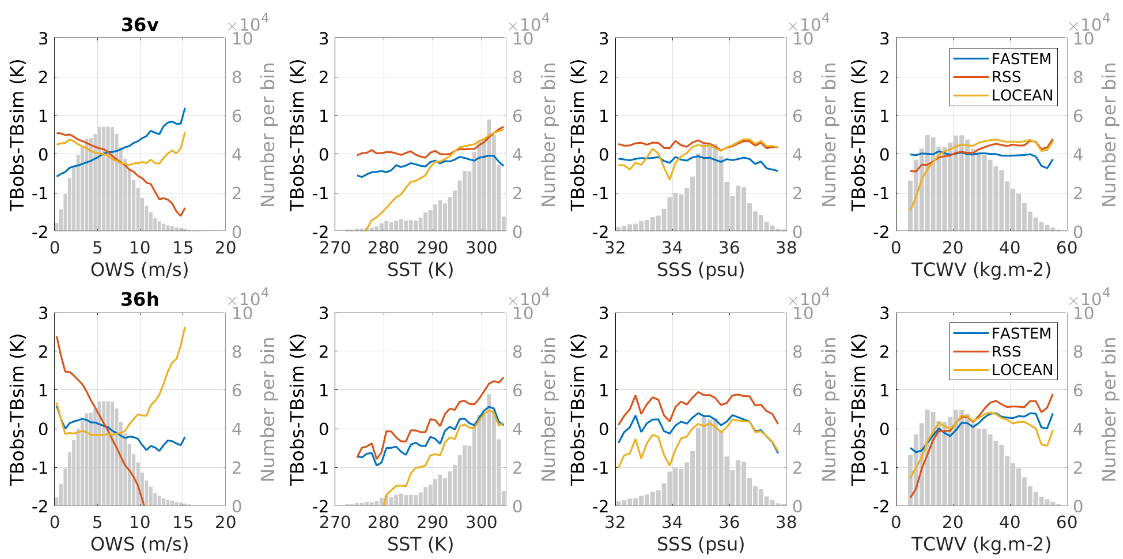

Figure 6: Same as Figure 3 but at 36.5 GHz.

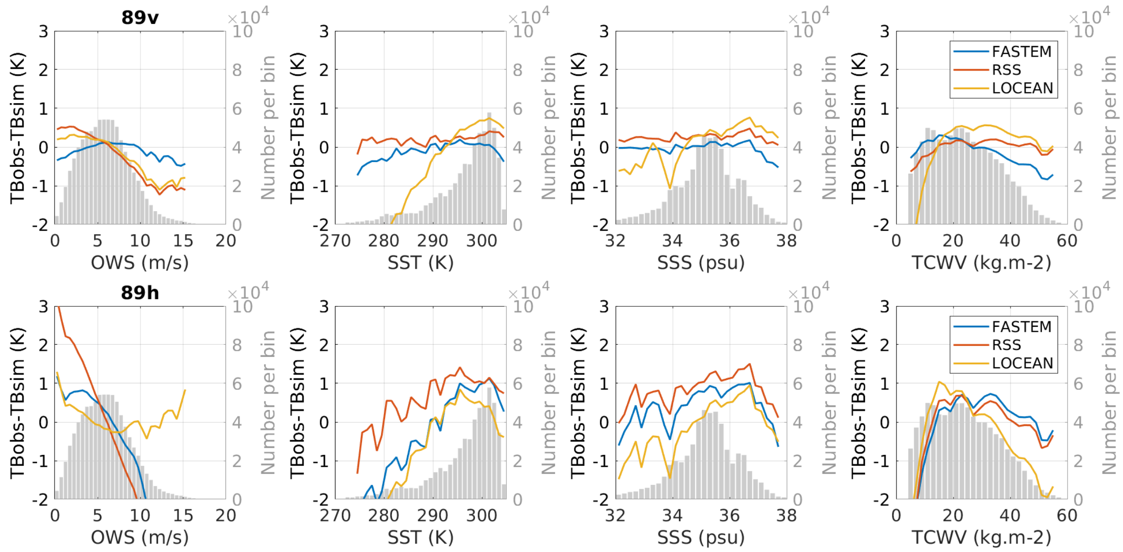

Figure 7: Same as Figure 3 but at 89 GHz.

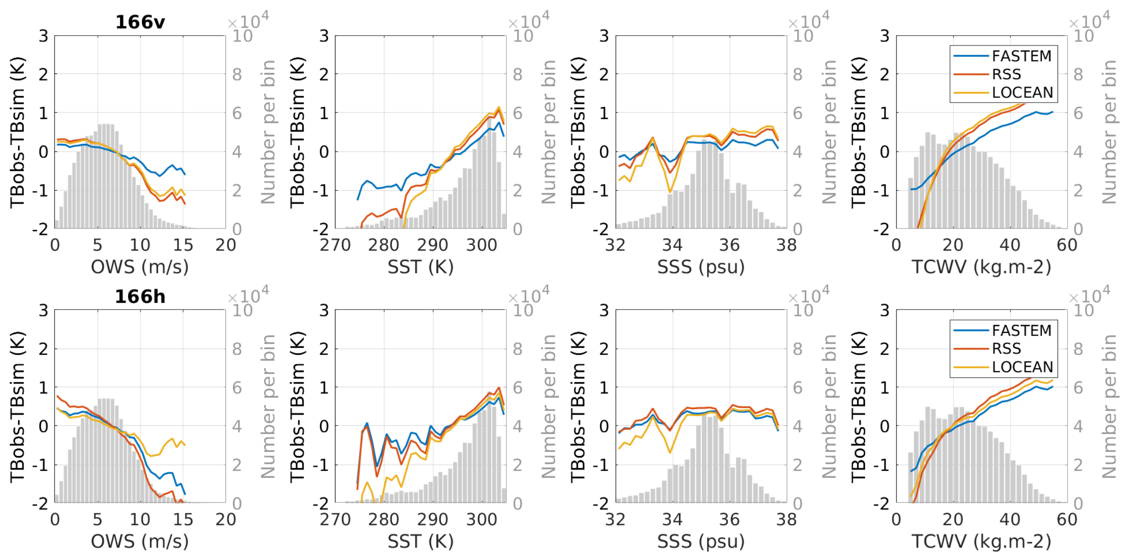

Figure 8: Same as Figure 3 but at 166.5 GHz.

5 Refinements needed to LOCEAN RTM

The LOCEAN RTM is a full physically-based model. It has been implemented by Emmanuel Dinnat [Dinnat et al., 2003], first of all for the analysis of L-band brightness temperatures (SMOS and SMAP), but it is very generic and can handle the complexity of a large range of situations. The model can simulate the 3^{rd} and 4^{th} Stokes composantes and it can take into account the wind speed direction. Recently, the capacity to simulate radar backscattering has also been added to this model. For all these reasons, this RTM has been selected as the reference quality model, during the ISSI workshop in 2019.

However, this physical model requires some updates for optimal application to higher frequencies. In the previous study with SMAP and AMSR2 observations [Kilic et al., 2019], it was concluded that the dielectric constant model and the foam model (foam emissivity and foam cover) were the major issues. The results obtained in this analysis with GMI observations confirm the first conclusions. In this section we analyze how these modules can be adapted.

5.1 Dependence to Sea Surface Temperature

Here, changes to the dielectric constants of LOCEAN model are tested. Dielectric constants of Klein and Swift [1977] have been replaced by the ones from Meissner and Wentz [2012] that are adequate for a larger range of frequencies. The dielectric constants from Meissner and Wentz [2012] are designed to work up to 90 GHz. Adjustments to extend this model to higher frequencies should be expected. The dielectric constants of FASTEM [Liu et al., 2011] are theoretically designed to work up to 410 GHz. However, they are expected to be less accurate than Meissner and Wentz [2012] for very low frequencies, as there is no specific efforts to adjust to these low frequencies.

Figure 9 illustrates these comparison results, in terms of TBs at the surface, for an OWS of 0 m/s and an incidence angle of 55°. With the dielectric constants from Meissner and Wentz [2012], the LOCEAN model matches almost perfectly the SST dependence of the RSS model, as at 0 m/s we are very close to the specular conditions and the Fresnel relations apply, as expected. These figures show the strong impact of the dielectric model on the surface TBs and the large differences induced in the TBs by the different formulations, with increasing frequencies. New dielectric measurements are underway at low microwave frequencies (mostly L-band). However, no effort is planed at high frequencies, despite the strong impact of this parameter with increasing frequencies. With increasing frequencies, the atmospheric transmission decreases and the limites the surface emissivity effect. However, in polar regions, the atmospheric transmission can be significant, and cold ocean conditions, discrepancies in the dielectric models could affect the simulated TBs.

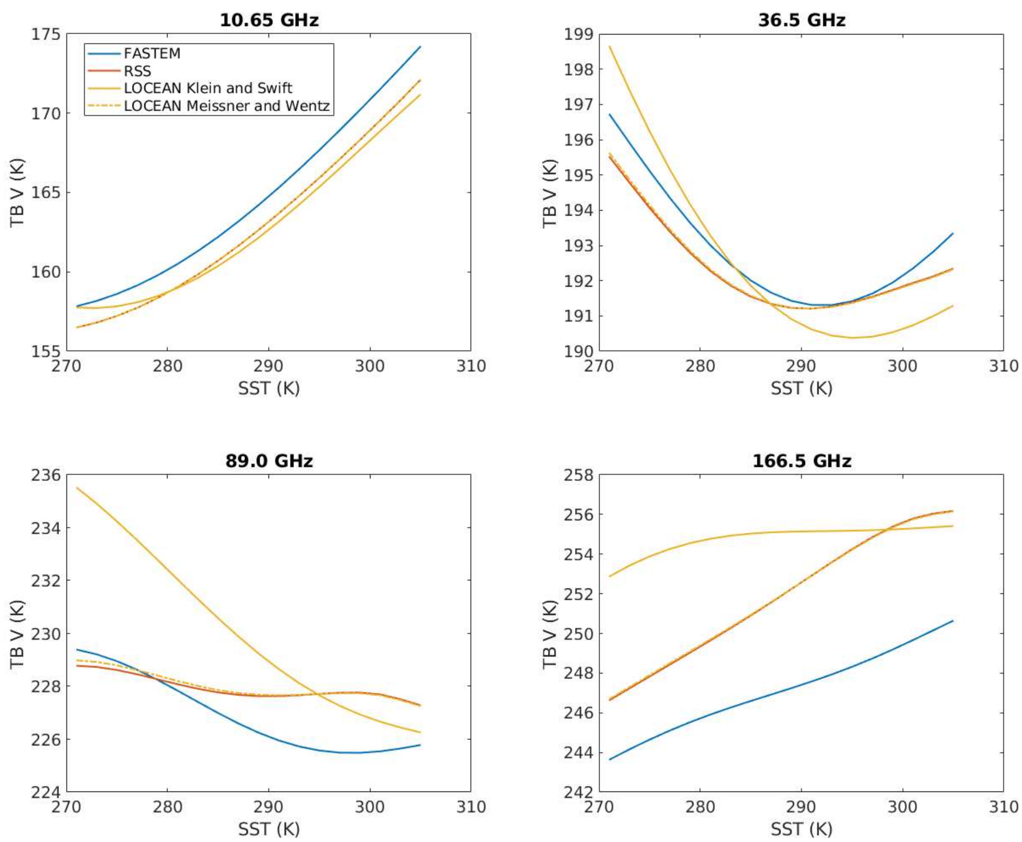

Figure 9: Surface brightness temperature of a flat sea (OWS = 0 m/s) as a function of the SST for channels at 10.65, 36.5, 89.0, and 166.5 GHz in vertical polarization for an incidence angle of 55° and a SSS of 34 psu.

5.2 Dependence to Ocean Wind Speed

Improving the OWS dependence of the LOCEAN RTM is complicated as the OWS dependance intervenes at different stages in the model, both in the wave spectrum as in the foam modeling. The OWS dependence is treated differently by the different models. RSS treats the OWS dependence with a single module which is the wind induced emissivity, whereas LOCEAN and FASTEM show OWS dependences in the wave spectrum, and in the foam cover. The foam emissivity also impacts indirectly the OWS dependence through the foam cover. Note that in this study, we have not yet dealt with the wind direction dependence.

In principle, foam appears at OWS > 7 m/s, meaning that below this value, only the wave spectrum affects the OWS dependence of the TB signal. LOCEAN RTM shows small errors (< 0.5 K) between 0 and 7 m/s meaning that the wave spectrum of Durden and Vesecky [1985] used in this model is likely suitable, even for high frequencies up to 166 GHz.

Foam is composed of whitecaps, bubbles, plumes, and sprays. It has a very complex and time-varying structure that makes modeling very difficult. During the ISSI meeting in November 2019, it was proposed to test the whitecap fraction as a function of different wind / wave parameters such as wave height or stability. The impact of spray was also discussed.

Given the complexity of the foam problem and the robustness that is expected from a reference model, how to deal with the foam in the reference emissivity model? The foam emissivity models such as Anguelova and Gaiser [2013] can very well describe the physical processes in the foam but microscopic or macroscopic parameters such as void fraction or foam thickness are required to run the model, and these parameters are clearly not easy to estimate, especially at global scale for NWP applications. On the opposite, wind-induced emissivity parameterization have been proposed, based on radiometric observations [Meissner and Wentz, 2012, Hwang et al., 2019], without trying to explain the physical processes. The recent paper by [Hwang et al., 2019] adopts a very pragmatic method to fit the observations at very high wind speed (even above 30 m/s).

One approaches could be to keep as much as possible the physical concepts at wind speeds below ∼15 m/s, and to bridge the gap toward a efficient parameterization such as in Hwang et al. [2019] for extreme high wind speed where the basic physical principles are very likely to fail. For this a good analysis of the different wave parameters is required.

For use of the sea surface emissivity models in NWP centers, it would be very attractive to keep the consistency with the physical ocean model. In that case, what are the ocean model parameters to be used for the sea surface emissivity modeling? Some preliminary tests have been performed to evaluate the variables of interest, available from ERA5 data. The wave parameters in ERA5 can be decomposed between wind waves (waves due to local wind) and swell (waves due to distant or delayed winds) or presented for the total sea (wind waves + swell). The short waves ($\lambda <$ 10-20 cm) essentially relate to the local wind, whereas the long gravity waves ($\lambda >$ 30 cm) can be related to distant wind. For more information about the ocean wave model at ECMWF, see Bidlot [2016] (wave-parameters.pdf).

Figure 10 presents the correlations between different parameters in the ocean wave ERA5 outputs: mean period of waves (wind waves only and total sea), the mean square slope (total sea), the peak wave period (total sea), and the significant height of waves (wind waves only and total sea). The wind speed, the mean period of wind waves, the mean square slope of waves, and the significant height of wind waves are highly correlated, showing that the number of parameters to use can be limited as they represent similar information.

The mean square slopes of the waves is of particular interest as it is directly used in most sea surface emissivity models, and is available from the ECMWF ocean model. Note that in the ocean model, this parameter is only representative of the wind waves, not of the swell. In Figure 11 the means square slopes from ERA5 are compared with the mean square slopes simulated with the expression from Cox and Munk [1954] and from FASTEM which use the expression of Cox and Munk [1954] and add a frequency dependence. We observe that the differences are large between the simulations and the reanalysis. The definition of the mean square slopes of waves can be very different, as some considered only the long wave, others considered both short and long waves and others define the mean square slopes depending on the radiometric frequency.

6 Conclusion and Perspectives

In this study, GMI observations have been compared with simulations from three RTMs: FASTEM, RSS, and LOCEAN from 10.65 to 166.5 GHz. This analysis is very close to the analysis performed with SMAP and AMSR2

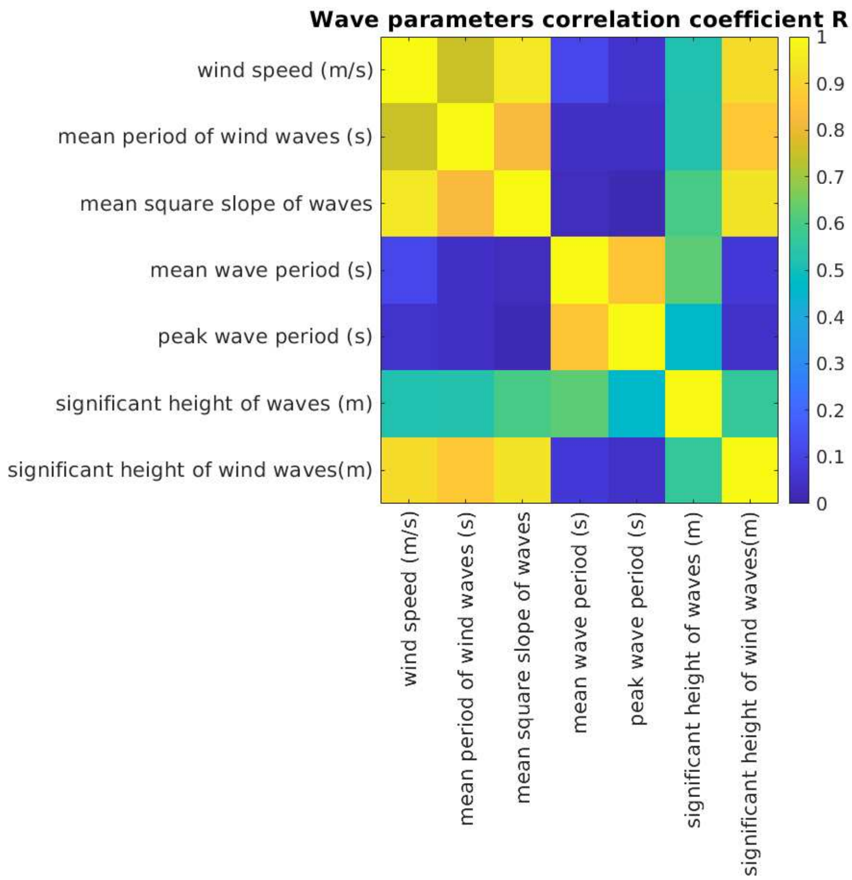

Figure 10: Correlation between wave parameters.

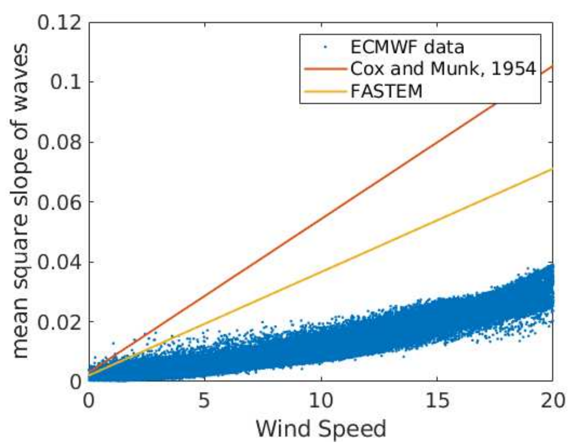

Figure 11: Mean square slopes of waves as a function of wind speed. For FASTEM simulations, the radiometric frequency is set to 18.7 GHz.

in Kilic et al. [2019]. The systematic errors obtained with GMI are small (<1.5 K with RSS and FASTEM) compared to the systematic errors obtained with AMSR2. It confirms the good calibration of GMI. For the errors observed as a function of the ocean parameters, the conclusions are similar than in the previous study: the major issues for the ocean RTM simulations are the high OWS and the low SST.

The LOCEAN RTM is a full physical model and is the best candidate to become the reference community model. It is currently adapted for L-band and is operationally used for SMOS. It requires some adjustments for better performances at higher frequencies. In the discussion, we showed that changing the dielectric constants could improve the LOCEAN RTM at higher frequencies, and reduce the errors observed at low SST. Lab measurements at high frequencies should be encouraged. Meanwhile, the dielectric constants from Meissner and Wentz [2012] can be used in the LOCEAN model, even if this dielectric model has not been specifically optimized to high frequencies.

For OWS dependence it is more complicated as all the RTMs show large errors for OWS > 7 m/s. A satisfying solution does not exist yet to improve this OWS dependence and efforts should be done in this direction. Recent parameterizations of the sea surface emissivity at very high wind speeds have been developed, from fits to radiometric observations. We will have to make sure that the physically-based reference emissivity model we want to develop can handle the high wind speed and we might have to bridge the gap between the physical model and the efficient parameterization for very high wind speeds.

In this study, the dependence of sea emissivity to wind direction has been ignored. The $3rd$ an 4^{th} Stokes composantes have not been analyzed yet, as they are not measured by GMI. In future work, this should be analyzed, as the signal due to wind direction is already implemented in the ocean RTM and the $3rd$ an 4^{th} Stokes composantes can be directly computed.

We also plan to analyze the incidence angle dependence by comparison between the Advanced Technology Microwave Sounder (ATMS) observations and ocean RTM simulations. ATMS is a cross-track sounder observing between 23.8 and 183.3 GHz. For this purpose, we will use L1B brightness temperatures from the ATMS onboard Suomi NPP provided by NASA at https://disc.gsfc.nasa.gov/datasets/SNPPATMSL1B_2/summary?keywords=ATMS.

The last version of the LOCEAN model implemented by Emmanuel Dinnat can simulate the radar backscattering. The active microwave observations are complementary with passive observations for OWS, as active observations are more sensitive to low OWS and passive observations to high OWS. This complementarity can be used to improve the RTM OWS dependence. In future works, we will analyze this active part of the RTM especially for the selection of a wave spectrum.

References

F. Aires, F. Marquisseau, C. Prigent, and G. Seze. A land and ocean microwave cloud classification algorithm derived from amsu-a and-b, trained using msg-seviri infrared and visible observations. *Monthly weather review*, 139(8):2347–2366, 2011.

M. D. Anguelova and P. W. Gaiser. Microwave emissivity of sea foam layers with vertically inhomogeneous dielectric properties. *Remote Sens. Environ.*, 139:81–96, 2013. ISSN 00344257.

J.-R. Bidlot. Ocean wave model output parameters. Technical report, ECMWF, 2016. URL https://confluence.ecmwf.int/download/attachments/59774192/wave_parameters.pdf?version=1.

C. Cox and W. Munk. Measurement of the Roughness of the Sea Surface from Photographs of the Sun's Glitter. *J. Opt. Soc. Am.*, 44(11):838–850, 1954. ISSN 00303941.

P. Debye. *Polar molecules,*. The Chemical Catalog Company Inc., New York, 1929.

E. P. Dinnat, J. Boutin, G. Caudal, and J. Etcheto. Issues concerning the sea emissivity modeling at L band for retrieving surface salinity. *Radio Science*, 38(4), aug 2003. ISSN 00486604.

S. L. Durden and J. F. Vesecky. A Physical Radar Cross-Section Model for a Wind-Driven Sea with Swell. *IEEE J. Ocean. Eng.*, 10(4):445–451, 1985. ISSN 15581691.

W. Ellison, A. Balana, G. Delbos, K. Lamkaouchi, L. Eymard, C. Guillou, and C. Prigent. New permittivity measurements of seawater. *Radio science*, 33(3):639–648, 1998.

S. J. English and T. J. Hewison. Fast generic millimeter-wave emissivity model. In *Microwave Remote Sensing of the Atmosphere and Environment*, volume 3503, pages 288–301. International Society for Optics and Photonics, 1998.

S. Favrichon, C. Prigent, C. Jimenez, and F. Aires. Detecting cloud contamination in passive microwave satellite measurements over land. *Atmospheric Measurement Techniques*, 12(3):1531–1543, 2019.

P. A. Hwang, N. Reul, T. Meissner, and S. H. Yueh. Ocean surface foam and microwave emission: Dependence on frequency and incidence angle. *IEEE Transactions on Geoscience and Remote Sensing*, 57(10):8223–8234, 2019.

M. Kazumori, Q. Liu, R. Treadon, and J. C. Derber. Impact Study of AMSR-E Radiances in the NCEP Global Data Assimilation System. *Mon. Weather Rev.*, 136(2):541–559, feb 2008.

L. Kilic, C. Prigent, J. Boutin, T. Meissner, S. English, and S. Yueh. Comparisons of ocean radiative transfer models with smap and amsr2 observations. *Journal of Geophysical Research: Oceans*, 2019.

L. Kilic, C. Prigent, F. Aires, G. Heygster, V. Pellet, and C. Jimenez. Ice concentration retrieval from the analysis of microwaves: A new methodology designed for the copernicus imaging microwave radiometer. *Remote Sensing*, 12(7):1060, 2020.

L. Klein and C. Swift. An improved model for the dielectric constant of sea water at microwave frequencies. *Oceanic Engineering, IEEE Journal of*, 2(1):104–111, 1977. ISSN 0364-9059.

J.-M. Lellouche, O. Legalloudec, C. Regnier, B. Levier, E. Greiner, and M. Drevillon. Quality information document for global sea physical analysis and forecasting product global analysis forecast phy 001 024. Technical Report Issue: 2.1, EU Copernicus Marine Service, 2019. URL http://cmems-resources.cls.fr/documents/QUID/CMEMS-GLO-QUID-001-024.pdf.

Q. Liu, F. Weng, and S. J. English. An improved fast microwave water emissivity model. *IEEE Transactions on Geoscience and Remote Sensing*, 49(4):1238–1250, 2011. ISSN 01962892.

T. Meissner and F. Wentz. The complex dielectric constant of pure and sea water from microwave satellite observations. *IEEE Trans. Geosci. Remote Sens.*, 42(9):1836–1849, sep 2004. ISSN 0196-2892.

T. Meissner and F. J. Wentz. The Emissivity of the Ocean Surface Between 6 and 90 GHz Over a Large Range of Wind Speeds and Earth Incidence Angles. *IEEE Trans. Geosci. Remote Sens.*, 50(8):3004–3026, aug 2012. ISSN 0196-2892.

T. Meissner, F. J. Wentz, and L. Ricciardulli. The emission and scattering of l-band microwave radiation from rough ocean surfaces and wind speed measurements from the aquarius sensor. *Journal of Geophysical Research: Oceans*, 119(9):6499–6522, 2014.

T. Meissner, F. Wentz, and D. Le Vine. The salinity retrieval algorithms for the nasa aquarius version 5 and smap version 3 releases. *Remote Sensing*, 10(7):1121, 2018.

E. C. Monahan and I. O'Muircheartaigh. Optimal Power-Law Description of Oceanic Whitecap Coverage Dependence on Wind Speed. *J. Phys. Oceanogr.*, 10(12):2094–2099, dec 1980. ISSN 0022-3670.

E. C. Monahan and I. G. O'Muircheartaigh. Whitecaps and the passive remote sensing of the ocean surface. *Int. J. Remote Sens.*, 7(5):627–642, may 1986.

C. Prigent, L. Kilic, F. Aires, V. Pellet, and C. Jimenez. Ice concentration retrieval from the analysis of microwaves: Evaluation of a new methodology optimized for the copernicus imaging microwave radiometer. *Remote Sensing*, 12(10):1594, 2020.

P. W. Rosenkranz. Line-by-line microwave radiative transfer (non-scattering), 2017.

R. Saunders, M. Matricardi, and P. Brunel. *A fast radiative transfer model for assimilation of satellite radiance observations-RTTOV-5*. ECMWF Reading, UK, 1999.

R. Saunders, J. Hocking, E. Turner, P. Rayer, D. Rundle, P. Brunel, J. Vidot, P. Roquet, M. Matricardi, and A. Geer. An update on the rttov fast radiative transfer model (currently at version 12). *Geoscientific Model Development*, 11(7):2717–2737, 2018.

A. Stogryn. The emissivity of sea foam at microwave frequencies. *Journal of Geophysical Research*, 77(9):1658–1666, 1972.

F. J. Wentz and D. Draper. On-orbit absolute calibration of the global precipitation measurement microwave imager. *Journal of Atmospheric and Oceanic Technology*, 33(7):1393–1412, 2016.

T. Wilheit and A. Chang. An algorithm for retrieval of ocean surface and atmospheric parameters from the observations of the scanning multichannel microwave radiometer. *Radio Science*, 15(3):525–544, 1980.

X. Yin, J. Boutin, N. Martin, and P. Spurgeon. Optimization of L-Band Sea Surface Emissivity Models Deduced From SMOS Data. *IEEE Transactions on Geoscience and Remote Sensing*, 50(5):1414–1426, may 2012. ISSN 0196-2892.

X. Yin, J. Boutin, E. Dinnat, Q. Song, and A. Martin. Roughness and foam signature on smos-miras brightness temperatures: A semi-theoretical approach. *Remote sensing of environment*, 180:221–233, 2016.

S. Yueh. Modeling of wind direction signals in polarimetric sea surface brightness temperatures. *IEEE Transactions on Geoscience and Remote Sensing*, 35(6):1400–1418, 1997. ISSN 01962892.